Recent Experiments with ECRH/ECCD in T-10.

The T-10 Team (presented by D.A. Kislov).

RRC ″Kurchatov Institute″, Moscow, Russia

e-mail contact of main author: notkin@nfi.kiae.ru

Abstract. Experiments with ECRH performed during 1998-2000 are presented. An operating regime with an edge transport barrier, interpreted as the H-mode, has been studied with both on-axis and off-axis ECRH. Experimental data imply formation of an internal transport barrier simultaneously with the external transport barrier in the case of off-axis ECRH. Strong evolution of plasma potential in the regions of the external and internal transport barriers has been observed using Heavy Ion Beam Probe diagnostics. The mode of improved confinement with peaked density profiles and increased ion temperature has been observed after pellet injection into ECRH heated plasmas. Experimental study of q(r) profile control by ECCD has been performed. Instabilities, identified as the neoclassical tearing modes, have been found to limit beta in the regimes with a high fraction of bootstrap current. The dependence of the critical β on the q(r) profile has been observed. A systematic study of plasma turbulence has been started using Correlation Reflectometry diagnostics.

1. Introduction

Experiments with ECRH/ECCD in T-10 performed during the period 1998-2000 are presented. T-10 is a tokamak with circular cross-section (at the present time with $B_T \leq 3$T and $I_p \leq 0.5$ MA, R=1.5 m, a=0.3 m) that started its operations in 1975. ECRH is the sole auxiliary heating method in T-10.

At present, the ECRH system [1], which consists of four gyrotrons (140 GHz, the second harmonic of EC frequency), provides up to 1.4 MW of injected power with a pulse length up to 0.4 s. The power is injected from the low magnetic field side in the extraordinary mode. Power injection at a toroidal angle of 21° to the major radius is used for ECCD. The orientation of the launching mirrors, which determines the injection angle, is fixed. Each gyrotron is equipped with a polarizer that allows injection of the elliptically polarized wave.

The characteristic feature of the T-10 tokamak is the pure electron heating provided by the ECRH system. An advantage of ECRH is its excellent localization. The half-width of the power absorption profile in the conditions of the experiments is about 10% of the minor radius. The cut-off electron density is $n_e = 7\times10^{19} m^{-3}$ in the conditions of oblique injection (from ray tracing calculations). This allows us to use ECRH without appreciable refraction with densities close to the Greenwald limit under $q_a \geq 4$. Power densities up to 8 W/cm^3 have been achieved in the core region. The density of power transferred from electrons to ions in the plasma core is much lower (by more than order of magnitude) than ECRH power density, which results in $T_e(0)/T_i(0) \sim 4\text{-}8 >> 1$. The ECRH system allows us to drive the current up to 70 kA with an efficiency close to that predicted by the TORAY code (up to $\eta_{CD} = I_p n_{e20} R/P_{ECRH} = 0.013 A/Wm^2$ in the conditions of T-10) [2].

Thus, a wide range of actual physical problems can be studied applying ECRH in T-10 experiments: The pure electron heating allows us to perform confinement studies in the conditions of hot electron component. Highly localized ECRH and ECCD make possible the control of MHD instabilities by the influence on the local parameters in the vicinity of a rational surface. A wide range of q(r) profiles in steady state, including ″advanced″

configurations with reversed magnetic shear (RMS), can be produced using ECCD [3]. This allows confinement and MHD stability studies in the conditions of different q(r) configurations. Thus, some experiments performed in 1990-1997 were aimed at investigation of ECCD physics [2,4], stabilization of sawtooth oscillations and tearing modes by ECRH/ECCD [5,6,7], and the physics of the density limit in plasmas with ECRH [8,9,10]. The main experiments with ECRH over the period 1998-2000 were aimed at the search for and investigation of modes of improved confinement under the conditions of hot electron component ($T_e >> T_i$) and investigation of MHD stability in the regimes with a high fraction of bootstrap current. It is worth mentioning the Heavy Ion Beam Probe diagnostics (HIBP) and Correlation Reflectometry diagnostics as the tools used to study the nature of transport and of physical processes leading to the transition to improved confinement regimes.

2. Regimes with the features of H-mode

Regimes with a spontaneous increase of stored energy that follows a sudden drop of D_α emission have been observed under ECRH [11, 12]. This is believed to be the same phenomenon as the H-mode. Strong evolution of plasma potential [13] and significant changes in plasma turbulence have been observed in the region of the external transport barrier in these regimes. A difference in $T_e(r)$ profile evolution after the D_α drop under on-axis and off-axis ECRH has been observed. Experimental data imply formation of an internal transport barrier simultaneously with the external transport barrier in the case of off-axis ECRH [12].

In the case of on-axis ECRH the transition to the regime that has the features of the H-mode (further - the L-H transition) is characterized by a sudden drop of D_α emission together with the start of the increase of the electron density, $\bar{n}_e$ (*FIG.1*). Both relatively ″fast″ (with the timescale of the D_α drop ~10 ms) and ″slow″ (~100 ms) transitions have been observed. An increase of the electron density (in spite of the switch-off of the gas puffing) starts together with the D_α drop. The density increase is accompanied by an increase of the density gradient near the limiter (*FIG.2*). This allows us to suppose formation of the edge transport barrier. The energy confinement time increases by a factor of ≤1.7. Fast L-H-L-like transitions have been observed from the D_α emission in some of the shots at the beginning of the increase of the stored energy. So far ELMs have not been observed in these regimes. The increase of the stored energy is associated mainly with the improvement of the particle confinement in the regimes with on-axis ECRH. The electron temperature profile changes insignificantly in this case. We note that in the conditions of T-10 plasmas with ECRH, when electron transport losses dominate, the energy confinement increases linearly with density [14]. Thus, the confinement in the H-mode-like regime was found to be close to that in the T-10 L-mode at the same density. The value of the threshold power for the transition (around 0.6 MW) was found to be consistent with ITER scaling [15] $P_{th}^{ITER} = 2.84 \cdot M^{-1} \cdot B_T^{0.82} \cdot \bar{n}^{0.58} \cdot R \cdot a^{0.81}$.

The evolution of the radial distribution of plasma potential in the outer part of the plasma column ($\rho = r/a \geq 0.4$) during the L-H transitions was measured by HIBP [16]. The evolution of the potential profile was measured by periodic (50 Hz) radial scans. The time interval between the potential profiles was 20 ms, the scanning time 4-7ms. The evolution of the plasma potential during and after L-H transition with a ″slow″ D_α drop is shown in *FIG.3*. A gradual decrease of plasma potential occurs near the limiter during the D_α drop that corresponds to negative (directed inward) changes of the radial electric field. During the D_α drop the ″potential well″ is formed, but finally in some of the shots the distribution of the potential

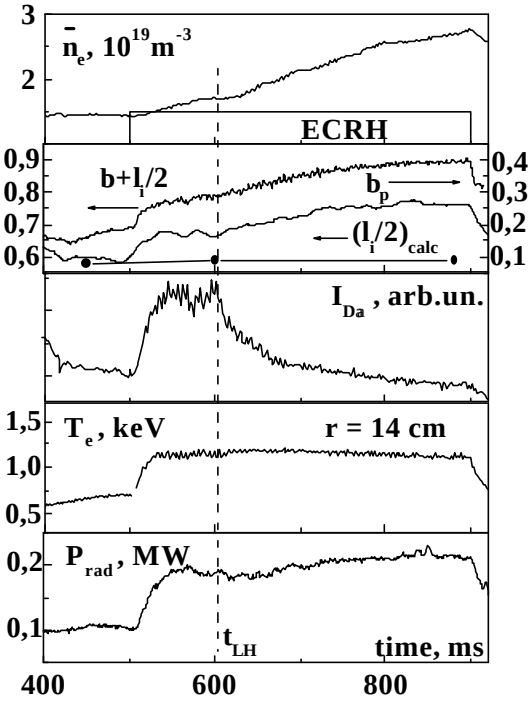

FIG. 1. Waveforms of $\bar{n}_e$, $b_p+l_i/2$, b_p (diamagnetic measurements), I_{Da} , T_e(14 cm) and radiation losses P_{rad}. The broken line marks the start of the transition.

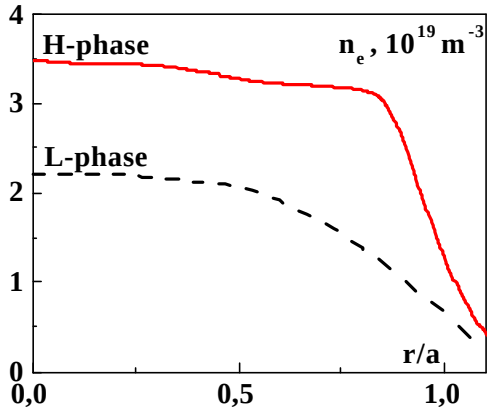

FIG. 2. Density profiles before and after the L-H transition.

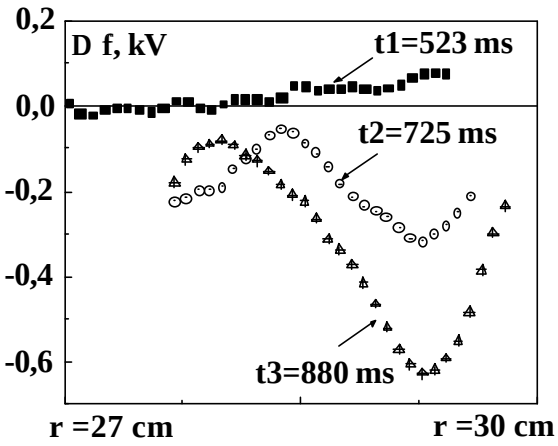

FIG. 3. Evolution of plasma potential during the $\bar{n}_e$ increase (see FIG. 1).

becomes monotonic. A narrow region (~1-2 cm) near the limiter with a strong drop of plasma potential (with $\Delta\varphi\approx300\div400$ V) is formed during the transition phase. The D_α intensity drop and the potential decrease starts simultaneously (within the accuracy of the measurements). We note that the observed evolution of the plasma potential is similar to the potential change during the L-H transition observed in JFT-2M using the HIBP diagnostic [17]. A decrease of T_e and plasma potential in the SOL during L-H transition has been observed in T-10 by the Langmuir probes [18].

In the case of off-axis ECRH the power was absorbed in the region around $\rho\approx0.6$. Unlike the regimes with on-axis ECRH, besides the $\bar{n}_e$ increase, a considerable increase in T_e in the plasma core (up to 30%) has been observed after the L-H transition (*FIG.4*). Thus, a considerable contribution of T_e to the increase of the stored energy occurs. The increased T_e gradient near $\rho\sim0.6$ has been observed after the L-H transition (*FIG.4,(a)*). According to estimations ion energy confinement time increases by up to a factor of 1.5. Evolution of plasma potential similar to that one observed in the edge during the L-H transition has been observed in the region of the increased T_e gradient (*FIG.4,(b)*). At first, a transient negative ″potential well″ is formed. Later the well is transformed to the distribution of potential with a

decrease near ρ~0.5. These features indicate the formation of an internal transport barrier together with the edge transport barrier in those shots.

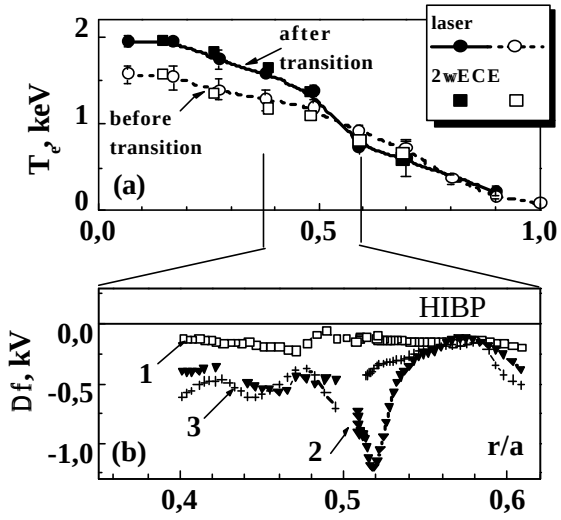

FIG. 4. (a) Electron temperature profiles before and after ITB formation, measured by Thomson scattering and ECE diagnostics.
(b) profiles of plasma potential before (1), during (2) and after (3) ITB formation.

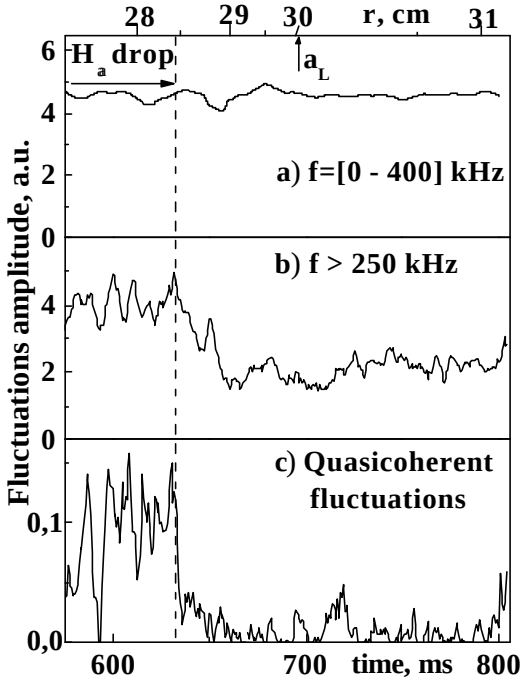

FIG. 5. Plasma turbulence evolution during L-H transition.

Plasma turbulence was investigated with the ordinary mode Correlation Reflectometry [19] in the regimes with the L-H transitions. According to the measurements, the amplitude of high frequency (>200 kHz) plasma turbulence decreases in the region of the edge transport barrier (r≥28.5 cm) with almost unchanged low frequency turbulence (*FIG.5*). ″Quasi-coherent″ fluctuations disappear after the D_α drop. Thus, the transition from the characteristic ″core″ turbulence spectrum to the SOL-like one occurs in the barrier region due to the reduction of the high frequency turbulence and disappearance of the ″quasi-coherent″ turbulence. (For a discussion on the types of fluctuations in the turbulence spectra, see Section 7.) Furthermore, the reduction of both radial and poloidal correlation length of the turbulence has been observed in the edge barrier region in H-mode (by a factor of ≈5), which is possibly responsible for the local decrease of transport. At the same time, an increase of the poloidal correlation length in the SOL region has been observed. The amplitude and the spectra of the plasma turbulence remain almost unchanged in the inner region.

The leading hypothesis for explanation of the L-H transition is E×B shear suppression of the turbulence that dominates the transport. We have observed the potential evolution together with the significant changes in plasma turbulence in the experiments. It is consistent with this general point of view. However, the physical processes leading to evolution of the E_r required for the transition are not quite clear yet. We have not observed an evolution of the plasma potential prior to the L-H transition within the accuracy of the measurements. A gradual decrease of the plasma potential together with a smooth turbulence reduction in the case of a ″slow″ D_α intensity drop allows us to suppose the partial suppression of the turbulence that dominates the transport in this case. The nature of the increased T_e gradient in the regimes with off-axis ECRH is not quite clear yet. However, changes of plasma potential similar to

that observed in the plasma edge could increase the E×B shearing rate that suppresses the turbulence and this could lead to the formation of the internal transport barrier.

3. Regime with improved confinement produced by deuterium pellet injection into an ECRH plasma

The transition to the regime with enhanced confinement (the pellet enhanced confinement (PEC) mode) after injection of a deuterium pellet into an ECRH plasma has been observed [20]. This mode is characterized by a peaked $n_e(r)$ profile and increased T_i. The global energy confinement time (τ_E) is restored to its ohmic value with the available P_{ECRH} in the best shots. The experiments have been performed in the regimes with $q_a \approx 2.5\text{-}3.5$, $\bar{n}_e \approx (3\text{-}4)\times 10^{19}$ m^{-3} and absorbed power (P_{ab}) up to 0.7 MW.

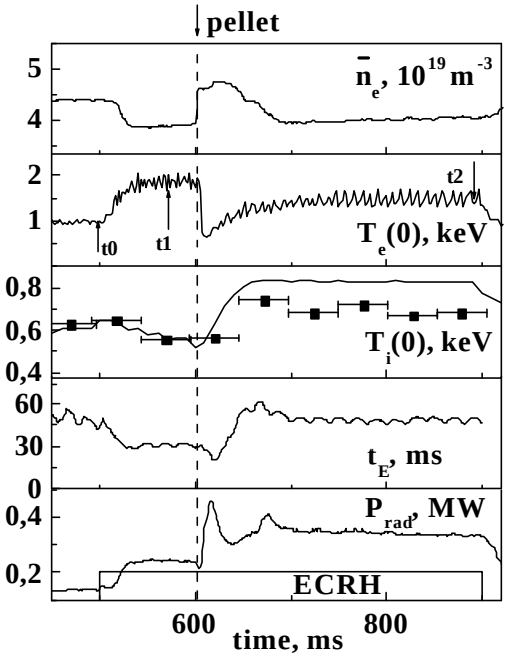

FIG. 6. Waveforms of $\bar{n}_e$, $T_e(0)$, $T_i(0)$ (from charge exchange and from neutron rate), t_E, and radiation losses P_{rad}.

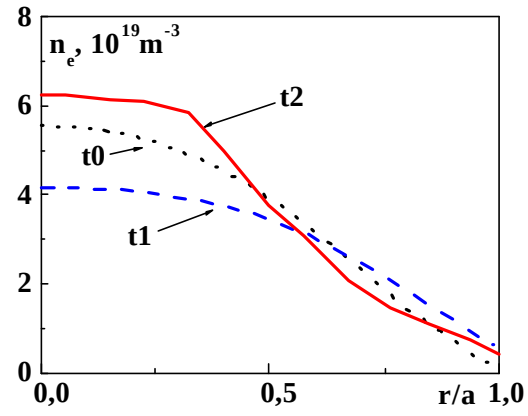

FIG. 7. The $n_e(r)$ profiles in OH, before and after the transition (see arrows in FIG. 6).

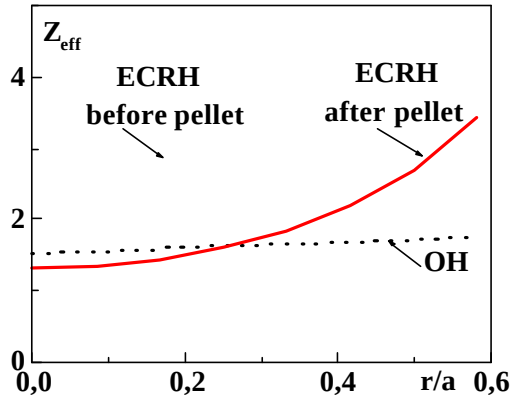

FIG. 8. Z_{eff} profiles in OH, before and after the transition.

The transition to the PEC mode occurs after the pellet injection. After an abrupt density increase due to the injected pellet, the line averaged electron density relaxes slowly to its pre-injection value (*FIG.6*), but the density profile remains peaked up to the end of the ECRH pulse (*FIG.7*) (for a period of 6-10τ_E). The density peaking factor increases from $n_e(0)/\langle n_e\rangle = 1.2$ before the pellet injection to $n_e(0)/\langle n_e\rangle = 1.8$ after the injection. Central T_i increases by ≈30%. The electron temperature after the abrupt drop due to the pellet injection

increases to a value that is lower by ≈20-30% than the pre-injection value. The profile of the electron temperature remains almost unchanged. The profile of Z_{eff}, estimated using the visible continuum data, is flat before the pellet injection. The value of Z_{eff} decreases in the plasma core and increases in the outer region after the pellet injection (*FIG.8*). The radiation losses increase by 30% and P_{rad}/P_{tot} attains the value of 0.4. (P_{rad} increases in the plasma periphery but decreases in the plasma core.)

According to D_α spectroscopy measurements an injected pellet is completely ablated in the outer part of the plasma ($\rho \geq 0.7$). A surprising feature is the timescale of the density and temperature cold pulse propagation into the plasma core. The temperature drop on a timescale of 0.1 ms was observed almost simultaneously in all ECE channels. Simultaneously with the T_e drop a density increase over the plasma column with a timescale of 0.1 ms has been observed. This timescale is two orders of magnitude lower than that expected from the diffusion coefficients. The transition occurs only in the shots with fast propagation of the cold pulse up to the plasma center. If the transition to the PEC mode does not occur, the profile of $n_e(r)$ becomes peaked but relaxes to the pre-injection state after the pellet injection (on a timescale ~100 ms). This occurs in OH, in the case of insufficient ECRH power or in the case of insufficient size of a pellet.

An outstanding feature of this regime is the restoration of the ohmic confinement in the plasmas with ECRH (with the available P_{ECRH}) that is sustained without signs of deterioration up to the end of the ECRH pulse (*FIG.6*). The energy confinement time τ_E in this improved mode increases with respect to τ_E without pellet injection by a factor of 1.6. A peaked $n_e(r)$ profile indicates increased particle confinement time τ_p in this regime.

It is worth noting some common features of the transition to the PEC mode in T-10 and the transition from L to RI-mode in TEXTOR [21]. The enhanced particle confinement results in significant peaking of the $n_e(r)$ profile. P_{rad}/P_{tot} increases due to the increase of P_{rad} in the plasma periphery. The value of $Z_{eff}(r)$ increases towards the plasma edge. The global energy confinement time increases considerably after the transition. Thus, some common mechanisms of confinement improvement in the observed regime and in RI mode could be supposed. The transition to the RI-mode in TEXTOR and the transition to the mode of improved confinement in our experiments have been satisfactorily described by the same model [22]. We note, that unlike the case of the transition into the RI-mode, the electron channel dominates the transport before pellet injection and τ_E has the same $\bar{n}_e$ dependence in T-10 as in the RI-mode. Further experimental and computational studies are required for understanding of the physical mechanisms leading to the transition and of the properties of the observed regime.

4. Studies of beta limitation by Neoclassical Tearing Modes

The limitation of the maximum achievable beta at a value well below the predictions of ideal MHD theory has been observed in T-10. Soft beta limits have been observed in plasmas with ECRH with high q_L (≈6-10). A significant fraction of bootstrap current (up to 50%) can be obtained in these regimes with high β_p (up to 2.5) and high l_i values (up to 2). The instabilities that are responsible for beta limitation in these experiments have been interpreted as Neoclassical Tearing Modes (NTMs) [23].

The β increase can be terminated by destabilization of the (3,2) or (2,1) mode. Waveforms of the shot suffered from destabilization of the (3,2) mode that terminates the smooth β increase, and later suffered from destabilization of the (2,1) mode, are shown in *FIG.9*. (A slow $\bar{n}_e$ increase during the ECRH pulse results in a β increase due to the linear dependence of τ_E on $\bar{n}_e$ in T-10 L-mode plasmas.) The mode onset results in a smooth degradation of confinement (with a decrease of the stored energy by up to 30%).

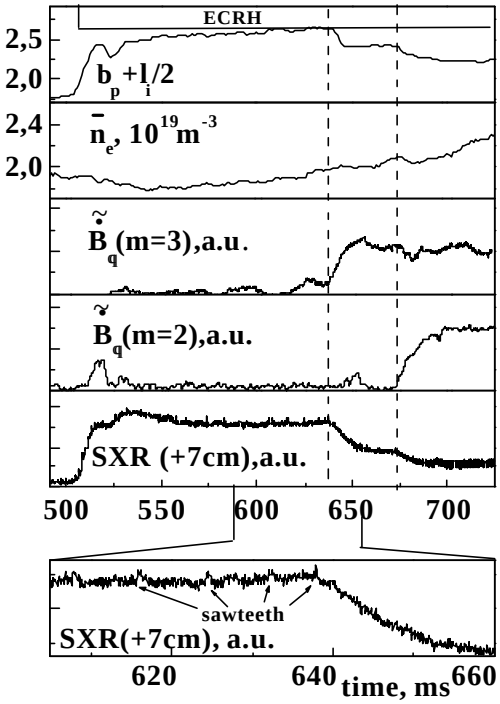

FIG. 9. Waveforms of the shot suffered destabilization of (3,2) and (2,1) modes. The (3,2) mode is triggered by a sawtooth.

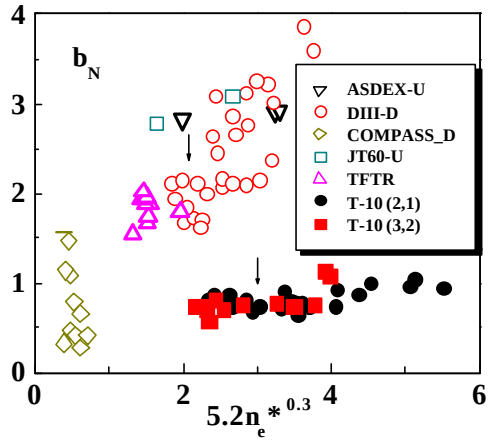

FIG. 10. b_N at NTM onset versus n_e^* ($n_e^*=0.012\ n_e(10^{20}m^{-3})qR(m)/e^{3/2}\ T_e^2(keV)$), $Z_{eff}=1$, the data on a resonance surface are used.

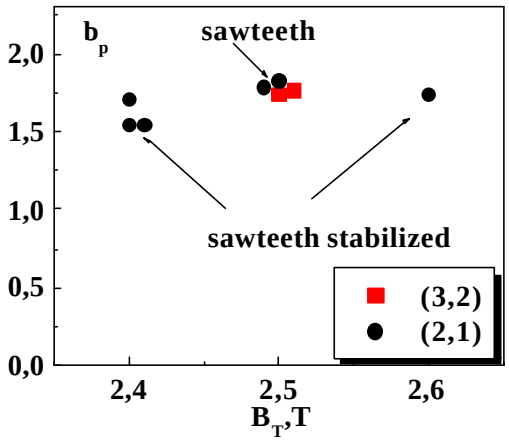

FIG. 11. Critical b in sawtoothing and sawtooth-free discharges.

The following features of the mode destabilization are consistent with NTM theory. The maximum achievable beta was limited at values well below the ideal limits. SXR oscillations observed after a soft β limit event have the characteristics of an island rotation. The stability analyses show that the development of a mode cannot be explained by evolution of the standard tearing mode stability parameter Δ_0'. The characteristic hysteresis effect [24] has been observed in T-10. Once destabilized, the mode persists throughout the discharge, in spite of the decrease of ECRH power to the value before the mode onset. We have found that a trigger (sawtooth) is always required for onset of the (3,2) mode.

As follows from *FIG.10* (the diagram is from Ref. [25]), the critical β_N in T-10 is well below the β_N values required for MHD onset in other devices with similar ν_e^*. We suppose that the main reason for this is that the beta limits have been obtained in the regimes with high q_a and high β_p. (The bootstrap current fraction sufficient for NTM onset could be obtained even with low β_N values in these regimes.) The critical β was found to be almost independent of ν_e^* in T-10 experiments (*FIG.10*). This effect could be explained in the framework of ion polarization current model. (Within this model, critical β depends on the factor $g(\varepsilon,\nu_{ii})$, which can be almost independent of collisionality if it is sufficiently low.) We note that the ρ^* value does not change appreciably in the T-10 experiments, thus any dependence of critical β on ρ^* has not been studied.

The experiment for clarifying the role of the sawtooth oscillations in NTM triggering in T-10 conditions has been performed. Off-axis co-ECCD has been applied for sawtooth suppression [26] in order to compare NTM thresholds with and without sawtooth oscillations. As is shown in *FIG.11*, the critical β_p is almost independent of the presence of sawtooth oscillations. It was found that either the (3,2) or the (2,1) mode can determine a soft beta limit event in the case of almost identical sawtoothing shots (as in the shots with sawteeth in *FIG.11*). However, in all the shots with sawteeth suppressed (under off-axis co-ECCD or on-axis counter-ECCD), the (2,1) mode determines a soft beta limit event. We suppose, that an evolution of Δ_0' during the ECRH pulse results in the formation of the seed island that is required for an NTM onset in the case without sawteeth. (According to stability calculations, Δ_0' for the (2,1) mode is usually marginal for the conditions of the experiments.) The Δ_0' parameter was found to be always negative for the (3,2) mode, thus a sawtooth trigger is required for the mode onset.

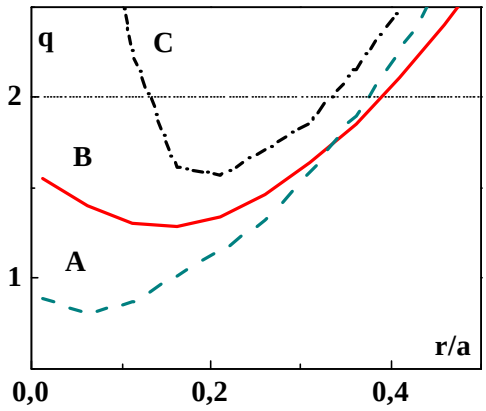

FIG. 12. Typical profiles of q(r) in the regimes with on-axis co- and counter-ECCD.

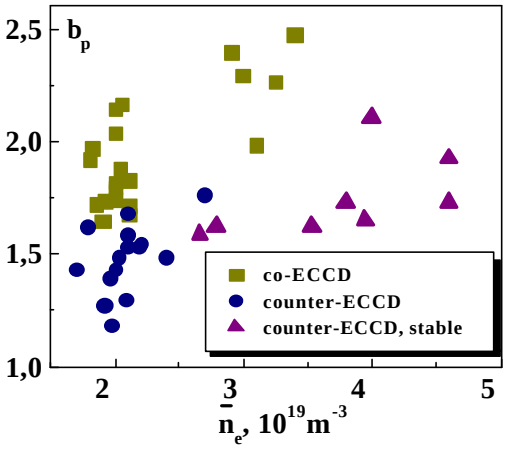

FIG. 13. Critical b_p versus $\bar{n}_e$ in the regimes with on-axis co- and counter ECCD.

The dependence of the critical β on the q(r) profile has been studied in the T-10 experiments. A wide spectrum of q(r) profiles with a range of q_{min} from ≤ 1 to ≈ 2.5 can be produced applying ECCD in the current flat-top [3]. *Fig. 12* shows typical profiles of q(r) for shots with on-axis co-ECCD (profile A) and on-axis counter-ECCD (profiles B,C for different power levels). (The q(r) profiles have been calculated by the ASTRA code [27] using the profile of the driven current from the TORAY code [28].) The value of β_p at MHD onset is systematically lower for the shots with on-axis counter-ECCD (q_{min} around 1.3) than in the shots with on-axis co ECCD ($q_{min} \leq 1$) (*FIG.13*). The shots with higher values of q_{min} (≥ 1.5) usually have two q=2 surfaces and MHD activity in these shots (which can be associated with double-tearing stability [3]) differs strongly from that one observed in a soft beta-limit event.

We do not take these shots into consideration. The shots with counter-ECCD without MHD (*FIG.13*) usually have q_{min} close to unity due to the higher values of $\bar{n}_e$ (lower ECCD efficiency). According to the calculations, the value of Δ_0' is higher for the shots with q_{min} around 1.3 than for the shots with q_{min} close to unity. We suppose that the observed difference of critical β for the regimes with co- and counter-ECCD can originate from a difference in Δ_0'. (According to NTM theory critical β can depend on the Δ_0' value.)

5. Investigation of plasma turbulence by Correlation Reflectometry

Studies of small-scale density fluctuations have been performed by the ordinary mode heterodyne correlation reflectometry [19]. It uses the reflection of the ordinary mode from the reflection layer where the plasma frequency is equal to the frequency of the incident wave. The method combines the advantages of high sensitivity to density fluctuations with availability of poloidal, radial and long distance toroidal correlation measurements. The correlation measurements are provided by two antenna arrays with a wide range of launching wave frequencies corresponding to cut-off densities of $(0.8\text{-}8)\times10^{19}m^{-3}$. The amplitude and the phase of the reflected wave have been measured using a sin-cosin detector in complex form or separately with a sampling rate up to 1 MHz (up to 8 reflectometry channels are available).

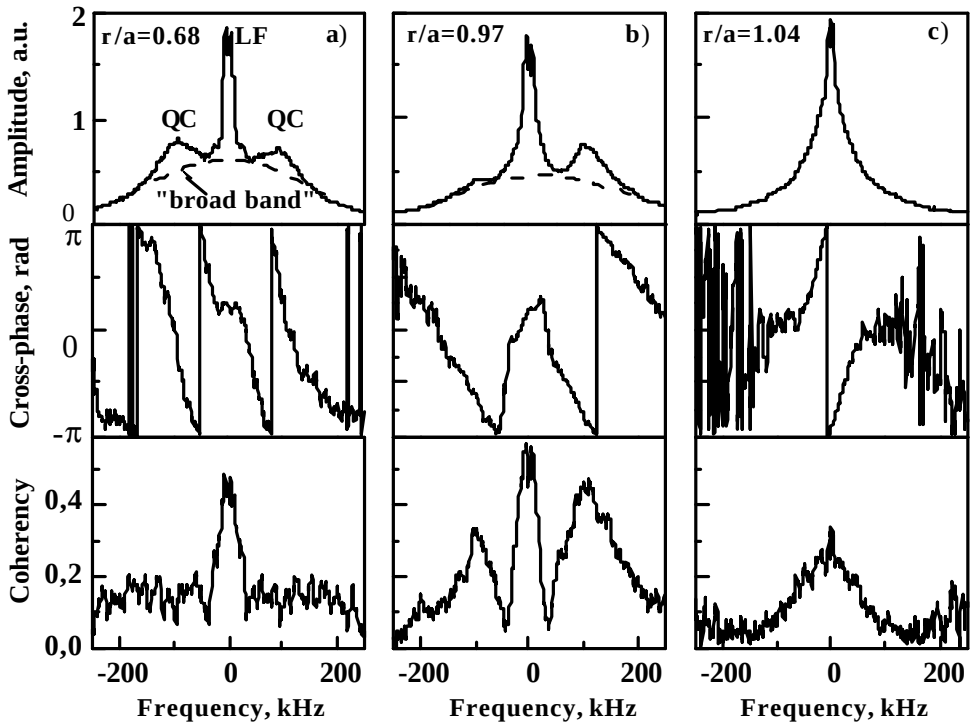

FIG. 14. Typical spectra of poloidal correlation reflectometry for three radial positions of reflection layer: central (a), periphery (b) and SOL (c).

The features of the plasma turbulence have been found to be qualitatively similar in OH, L and H-like modes. The results of poloidal cross-correlation analyses for three characteristic of plasma regions are shown in *FIG.14*: for the central part of the plasma column in (*a*), for the region outside $r_{q=2}$ in (*b*) and for the SOL in (*c*). The amplitude spectrum of a channel, the cross-phase and the coherency spectra between two channels are shown from top to bottom for each reflection region. The main features of the turbulence are the same across the plasma column (except the SOL region). The spectra shown in *FIG.14*,(*a*) and (*b*) have a common

appearance that is characterized by the ″quasi-coherent″ (QC) maxima near ±100 kHz, a low frequency (LF) maximum in the region of zero frequency and ″broad band″ fluctuations (shown by the dashed lines). According to Refs. [29, 30], a single instability could be a possible source of QC and ″broad band″ types of fluctuations. The possible role of these two types of fluctuations in the genesis of the LF fluctuations is under investigation. The phase velocity of LF turbulence, which is characterized by the slope of the cross-phase, differs across the plasma column (see *FIG.14*). LF fluctuations are fixed in laboratory frame in the central region (*FIG.14*,(*a*)), while in the outer region (*FIG.14*,(*b*)) they rotate in the ion diamagnetic direction. QC fluctuations rotate in all cases in the electron diamagnetic drift direction. Thus, the opposite rotation directions of LF and QC turbulence types in the plasma periphery were observed (*FIG.14*,(*b*)). The experiments for investigation of turbulence rotation relative to the plasma rotation are in progress now. It was shown earlier [31] that the rotation of QC fluctuations is close to the plasma rotation in the T-10 plasma core. The SOL turbulence (*FIG.14*,(*c*)) has a single component structure that is similar to that one measured by the Langmuir probes [32, 33]. It is concluded that the plasma turbulence in OH, L and H-like mode plasmas has qualitatively the same features across the plasma column, which differ from the features of the SOL turbulence.

6. Conclusion

The main results of the experiments with ECRH in T-10 over the period 1998-2000 are:

- The H-mode-like regimes have been studied with both on-axis and off-axis ECRH. Experimental data indicate formation of internal transport barrier simultaneously with the external transport barrier in the case of off-axis ECRH. The physical mechanisms of the transport barriers formation have been studied using Heavy Ion Beam Probe and Correlation Reflectometry diagnostics.

- The regime of improved confinement has been obtained using deuterium pellet injection into the plasma with ECRH. The regime is characterized by restoration of the ohmic confinement, that can be sustained up to the end of the ECRH pulse without degradation.

- Neoclassical Tearing Modes have been found to limit the beta value in high β_p regimes. A study of the dependence of critical β on plasma parameters in a wide range of operating regimes has been performed. The dependence of the critical β on the q(r) profile (modified by ECCD) has been observed.

- A systematic study of the plasma turbulence that dominates the transport in the conditions of hot electron component ($T_e >> T_i$) has been started using Correlation Reflectometry diagnostics.

7. Future plans

This section is focused on the future plans concerning experiments with ECRH in T-10. The gradual modernization of the T-10 ECRH system has been proposed. The first step of the modernization is transformation of the one-frequency system into a two-frequency system. A fifth gyrotron with a power of 0.5 MW at a frequency of 130 GHz, and then possibly at 150 GHz, will be applied in future experiments. Thus, on-axis and off-axis heating and current drive will be available simultaneously. The next step is the progressive increase of the power at 140 GHz (up to a doubling of the injected power). At the same time the launching system

will be modernized. Both oblique injection for ECCD and injection at zero toroidal angle for pure ECRH will be available. Thus, operation with considerably higher densities without refraction will be available in the case of pure ECRH.

Further investigation of confinement and stability properties of plasmas in a wide range of operating regimes with ECRH/ECCD will be performed. The main research topics of the future experiments are:

- Further investigation of the observed modes of improved confinement – the H-mode-like regimes and the improved mode with pellet injection. Transport mechanisms in these regimes will be studied. Special attention will be paid to the mode with pellet injection, the regime with the best performance in T-10.

- Studies of the neoclassical tearing mode beta limit in a range of operating regimes with a large fraction of bootstrap current. Investigation of NTM suppression by ECCD feedback modulation. The two frequency system will be applied in these experiments.

- The search for new regimes of improved confinement in T-10 will be continued with the modernized ECRH system. Studies of confinement and stability in the advanced scenario configurations are planned in the conditions of increased ECRH power.

- Confinement and stability properties of the regimes with $\bar{n}_e$ close to n_{Gr}. Experiments in the regimes with linear dependence of τ_E on $\bar{n}_e$ at high densities, as in the RI mode, are proposed.

This work was supported by the Ministry of Atomic Energy of Russia and by the Ministry of Science and Technology of Russia (Federal Program “Controlled Thermonuclear Fusion and Plasma Processes”).

References

[1] V.V.ALIKAEV et al., Fizika Plasmy, (1993) v. 19, No. 3, p. 291.
[2] YU.V.ESIPCHUK, Plasma Phys. Controll. Fusion, (1995) v.37, A267
[3] V.V.ALIKAEV et al., Plasma Phys. Reports, (2000) v. 26, No. 3, p.177.
[4] V.V.ALIKAEV et al., Nuclear Fusion, v.32 (1992) No. 10, p. 1811.
[5] D.A.KISLOV et al., in Proc. of 22 Conf. on Controlled Fusion and Plasma Physics, Bournemouth, (1995) v. 19C, Part I, p. 369.
[6] D.A.KISLOV et al, Nuclear Fusion, (1997) v. 37, No. 3, 339.
[7] N.V.IVANOV et al., in Proc. of 22 Conf. on Controlled Fusion and Plasma Physics, Bournemouth, (1995) v. 19C, Part III, p. 77.
[8] V.V. ALIKAEV et al., in Proc. of 17 Conf. on Controlled Nuclear Fusion and Plasma Heating, (1990), Amsterdam, ECA, v. 14B, part III, p. 1080.
[9] K.A.RAZUMOVA et al., in Proc. of 13 IAEA Conf. on Plasma Physics and Controlled Nuclear Fusion Research, Washington, 1990, V.1, p. 163.
[10] P.V.SAVRUKHIN et al., Nuclear Fusion, (1994) v.34, p. 317.
[11] YU.V.ESIPCHUK in Proc. of 18 IAEA Conf., 2000, Sorrento, Italy, EXP5/16.
[12] K.A.RAZUMOVA et al., Submitted to Plasma Physics Report.
[13] L.G. ELISEEV et al., to be published in Proceedings of 27 EPS Conference, June, 12-16, 2000, Budapest, Hungary.
[14] YU.V.ESIPCHUK, et al, J. Moscow Phys. Soc., (1991) No.1, p.119.

[15] Technical Basis for the ITER-FEAT Outline Design, Ch. 1, Sec. 2, p. 3.
[16] A.V.MELNIKOV, et al., 1999, 26 EPS Conf. Plasma Phys. Control Fusion, Maastricht, 23J, p. 829.
[17] Y.HAMADA et al., In Proc. of 17 IAEA Fusion Energy Conference, Yokohama, 1998.
[18] G.S.KIRNEV, S.A. GRASHIN, L.N. KHIMCHENKO, will be published in Czechoslovak Journal of Physics, (2000) Vol. 50, No 12.
[19] V.A.VERSHKOV, V.V.DREVAL, S.V.SOLDATOV, Review of Scientific Instruments, (1999), v. 70, p.1700.
[20] YU.D.PAVLOV et al., to be published in Proc. of 18 IAEA Conference, October 4-11, 2000, Sorrento, Italy (EXP5/17).
[21] J.ONGENA et al., in Controlled Fusion and Plasma Physics (Proc. 20 Eur. Conf., Lisbon, 1993), Vol 17C, Part 1, European Physical Society (1993) 127.
[22] YU.N.DNESTROVSKIJ, 26 EPS Conf. on Control. Fusion and Plasma Physics, Maastricht, ECA, vol.23J (1999), p.817.
[23] D.A.KISLOV et al., to be published in Proc. of 18 IAEA Conference, October 4-11, 2000, Sorrento, Italy (EXP3/04).
[24] H.ZOHM et al., Proc. 23 EPS Conf. on Control. Fusion and Plasma Physics, Kiev, v. 20C (1996), Part I, p. 369.
[25] O.SAUTER et al., Phys.Plasmas, (1997) v.4, No. 5, p.1654.
[26] D.A.KISLOV et al., Proc. 22 EPS Conference on Control. Fusion and Plasma Physics, Bournemouth (1995), v.19C, Part I, p. 369.
[27] G.V.PEREVERZEV et al., Kurchatov Institute Report IAE-5358/6, 1992.
[28] R.H.COHEN, Phys. Fluids (1988), v. 31, No. 6, p.421.
[29] F.ROMANELLI, F.ZONCA, Phys. Fluids, (1993) v. B5, p.4081.
[30] Z.LIN et al, Science, (1998) v.281, p.1835.
[31] V.A.VERSHKOV, et al., Nuclear Fusion, (1999), v.39, No. 11Y, p.1775.
[32] V.A.VERSHKOV et al., 21 EPS Conf., Montpellier 1994, v. 18B, Part 3, p. 1192.
[33] V.A.VERSHKOV et al., Journal of Nuclear Materials, (1997) v.241 – 243**,** p.873.